Human Molecular Genetics, 2020, Vol. 29, No. 9 1405–1416

doi: 10.1093/hmg/ddz185
Advance Access Publication Date: 2 September 2019
General Article

GENERAL ARTICLE

Tbx5 inhibits hedgehog signaling in determination of digit identity

Huiting Xu[1,3], Menglan Xiang[1], Yushu Qin[2], Henghui Cheng[2,4], Duohua Chen[2,5], Qiang Fu[1,4], Ke K. Zhang[2,6] and Linglin Xie[1,2,*]

[1]Department of Biomedical Sciences, University of North Dakota, Grand Forks, ND 58202, USA, [2]Department of Nutrition and Food Science, Texas A&M University, College Station, TX 77843, USA, [3]Hubei Cancer Hospital, Wuhan, Hubei 430079, China, [4]Tongji Hospital, Huazhong University of Science and Technology, Wuhan, Hubei 430030, China, [5]Department of Food Science, Changsha University, Changsha, Hunan 410078, China and [6]Center for Epigenetics & Disease Prevention, Institute of Biosciences & Technology, College of Medicine, Texas A&M University, Houston, TX 77030, USA

*To whom correspondence should be addressed at: Department of Nutrition and Food Sciences, Texas A&M University, TAMU 2253 College Station, TX 77843, USA. Tel: 979-862-9141; Email: Linglin.xie@tamu.edu

Abstract

Dominant TBX5 mutation causes Holt-Oram syndrome (HOS), which is characterized by limb defects in humans, but the underlying mechanistic basis is unclear. We used a mouse model with Tbx5 conditional knockdown in Hh-receiving cells (marked by Gli1+) during E8 to E10.5, a previously established model to study atrial septum defects, which displayed polydactyly or hypodactyly. The results suggested that Tbx5 is required for digit identity in a subset of limb mesenchymal cells. Specifically, Tbx5 deletion in this cell population decreased cell apoptosis and increased the proliferation of handplate mesenchymal cells. Furthermore, Tbx5 was found to negatively regulate the Hh-signaling activity through transcriptional regulation of *Ptch1*, a known Hh-signaling repressor. Repression of Hh-signaling through *Smo* co-mutation in Tbx5 heterozygotes rescued the limb defects, thus placing *Tbx5* upstream of Hh-signaling in limb defects. This work reveals an important missing component necessary for understanding not only limb development but also the molecular and genetic mechanisms underlying HOS.

Introduction

Digit patterning is controlled by the secretion of Sonic hedgehog (Shh) protein at the posterior limb bud mesoderm, in the zone of polarizing activity (ZPA). In mice, Shh is activated 12 h after the initiation of the limb bud (1), and Gli3 is required throughout limb development (1–5). Shh mediates patterning by regulating Gli, especially Gli3 protein, whose full length or truncated forms act as either an activator (Gli3A) or a repressor (Gli3R) of Shh. A proper ratio and expression pattern of Gli3A:Gli3R along the anterior–posterior axis specifies limb digit number and identity (3,5–8). Gain- and loss-of-function studies of Shh or Gli3 have shown phenotypes of syndactyly including polydactyly and oligodactyly, thus suggesting that Shh-signaling progressively controls digit formation, with more posterior identifies and in a dose-dependent manner (2,9–11).

Tbx5, a member of the T-box transcription factor family, plays a pivotal role in early cardiovascular morphogenesis. In humans, TBX5 haploinsufficiency causes Holt-Oram syndrome

Received: April 26, 2019. **Revised:** July 2, 2019. **Accepted:** July 18, 2019

(HOS), which is characterized by forelimb deformities, often together with congenital heart defects (12,13). In patients with upper limb anomalies, the abnormalities range from minor, such as syndactyly, to severe, such as reduction deformities (14). Digit abnormality is the most prevalent abnormality and includes both oligodactyly and polydactyly (14–18).

Tbx5 is essential in forelimb bud initiation, because Tbx5 knockout (KO) mice and zebrafish fail to form forelimbs (19–23). Tbx5 activates Fgf10 expression in the limb mesenchyme, which in turn activates Fgf8 expression in apical ectodermal ridge and supports continued limb outgrowth (20,22–25). Before Carnegie stage 15, TBX5 is expressed throughout the limb bud, and TBX5 expression extends into the presumptive thumb domain after Carnegie stage 16. There, the overlapping expression of Tbx5, Hoxa13, Gli3R and Hoxd13 defines the thumb domain (26–28). Tbx5 regulates Sall4 transcription, and the interaction of Tbx5 with Sall4 finely regulates patterning and morphogenesis of the anterior forelimb and the heart in both a positive and negative manner (28). This finding reveals a potential molecular and genetic mechanism for how Tbx5 mutation causes HOS. However, abnormalities in digit patterning have never been reported in Tbx5 mutant mouse embryos. Given that digit abnormality is the most common limb defect in HOS patients, the mechanistic basis of how Tbx5 mutations influence HOS remains to be clarified.

Our previous study has reported that Tbx5 acts upstream of Hh-signaling in the cardiac mesoderm and regulates the proliferation and cell cycle progression of cardiac progenitor cells, thus further contributing to the formation of the dorsal mesocardium protrusion for atrial septation (29). The interaction between Tbx5 and Hh-signaling during heart development suggests a potential role of those in limb development, which has yet to be elucidated. Here, we show that Tbx5 inhibits the Hh-signaling, thereby influencing digit patterning through regulation of *Ptch1* transcription.

Results

Tbx5 expression in the developing limb overlapped with the Hedgehog-receiving region

To investigate the potential interaction between Tbx5 and Hh-signaling pathways in limb development, we first examined the expression of both Tbx5 and the Hh-signaling responder, Gli1. At E10.5 and E12.5, the expression of Tbx5 in the developing limb was detected via immunohistochemical staining (IHC). In agreement with a previous report (20,23), Tbx5 expression was observed exclusively in the forelimb bud at E10.5 (Fig. 1A–D). Because Shh is known to be expressed in the limb from E9.5 to E11.5 and is required for limb growth and patterning during the first 12 h (1), we used genetic inducible fate mapping (GIFM), with induction by tamoxifen (TMX) administration at E8.5, to mark the Gli + limb precursor cells that receive Hh signals during limb patterning and growth. Through the Cre-inducible *lacZ* reporter *R26R* (30) with *Gli1Cre:ERT2*, cells responding to Hh-signaling and TMX were labeled on the basis of β-galactosidase expression. The location of marked Gli1+ progenitors was tracked through a time course analysis at E10.5. The Gli1+ progenitors and their descendant cells were limited at the proximal portion of the limb bud and more concentrated at the posterior–proximal limb bud and were found to overlap with the ZPA (Fig. 1E and F). Clearly, Tbx5 expression overlapped with the Gli1+ progenitors and their descendant cells at E10.5.

Disruption of Tbx5 expression in Hh-receiving limb precursors resulted in both polydactyly and oligodactyly

In our previous study, using *Gli1Cre:ERT2*, we found that TMX induces conditional Tbx5 haploinsufficiency in second heart field (SHF) Hh-receiving cells and results in high penetration (40%) of atrial septal defects (29). To study the interaction between Tbx5 and Hh-signaling in limb development, and to determine the ontogeny of HOS regarding both heart and limb malformation, we adopted the same strategy (TMX at E7.5 and E8.5) to simultaneously disrupt Tbx5 expression in the developing limb and in cardiac precursor cells. We confirmed significantly decreased expression of Tbx5 at E10.5 within the posterior limb bud (Fig. 2A–D), within the TMX interfering window from E8.0 to E10.5, whereas the expression of Tbx5 in the limb bud was not affected at E11.5 (Fig. 2E–H). These results confirmed that the TMX-induced Tbx5 abrogation affected only the limb mesenchymal cells from E8.0 to E10.5.

At E14.5, the $Tbx5^{fl/+}$ embryos displayed normally patterned limbs with five well-developed digits (97.0%, 160/165, Fig. 2I and J). The limb defects observed in five embryos (3% of total) might have resulted from mild TMX toxicity. However, 11.0% of the $Tbx5^{fl/+}$;*Gli1-CreER*$^{T2/+}$ embryos developed polydactyly (7/82) or oligodactyly (2/82) (Fig. 2K and L). In *Tbx5* KO ($Tbx5^{fl/fl}$; *Gli1-CreER*$^{T2/+}$) embryos, the incidence of digit abnormality was as high as 54.1% (Table 1, 60/111 total embryos, Fig. 2M and N). Among the abnormalities, polydactyly accounted for ~83.3% (50/60, Fig. 2M) and oligodactyly accounted for the remainder (Table 1, 10/60, Fig. 2N). The polydactyly occurred primarily at the first digit side (Table 1, 37/50, 74%, Fig. 2M, right hand), although additional digits were also found in other locations (Fig. 2M, left hand). A characteristic feature of HOS patients is that the left limb is more severely affected than the right (31). However, we did not observe a left–right difference on either the severity or the incidence of the digit defects in our Tbx5 mutant mouse model.

Tbx5 deletion inhibited the apoptosis of autopod mesenchymal cells associated with polydactyly

We wondered whether Tbx5 deletion might lead to increased cell death in the developing limb bud. Therefore, we examined cell apoptosis via TUNEL assays at E11.5 and E12.5. At E11.5, the morphology of the late-distal tissue in wild-type and mutant limb buds was indistinguishable, whereas at E12.5, the polydactyly or the oligodactyly was recognized. Apoptotic cells were counted from five serial sections, and the total numbers of TUNEL-positive cells in each embryo were analyzed with one-way ANOVA. At E11.5, we observed significantly fewer apoptotic cells at the center region of the proximal border of the handplate mesenchyme, previously recognized as the opaque patch in bird limb bud (32), in $Tbx5^{fl/fl}$;*Gli1-CreER*$^{T2/+}$ than in $Tbx5^{fl/+}$ embryos (Fig. 3A and B vs. C and D and Fig. 3E, 125 ± 20 vs. 66 ± 22, $P = 0.004$). At E12.5, programmed cell death was observed at the foyer preaxial primaire (*ffp*) in $Tbx5^{fl/+}$ embryos; however, the apoptotic cells in *ffp* were nearly absent in $Tbx5^{fl/fl}$;*Gli1-CreER*$^{T2/+}$ embryos with obvious polydactyly (Fig. 3G and J vs. F and I and Fig. 3L, 8 ± 4 vs. 65 ± 7, $P = 0.000017$). Interestingly, the $Tbx5^{fl/fl}$;*Gli1-CreER*$^{T2/+}$ embryos without polydactyly still displayed programmed cell death at this zone (Fig. 3H and K vs. F and I and Fig. 3L, 73 ± 12 vs. 65 ± 7, $P = 0.307$). Unfortunately, with the very low incidence of oligodactyly (<10% of all embryos), we were unable to collect enough replicates that

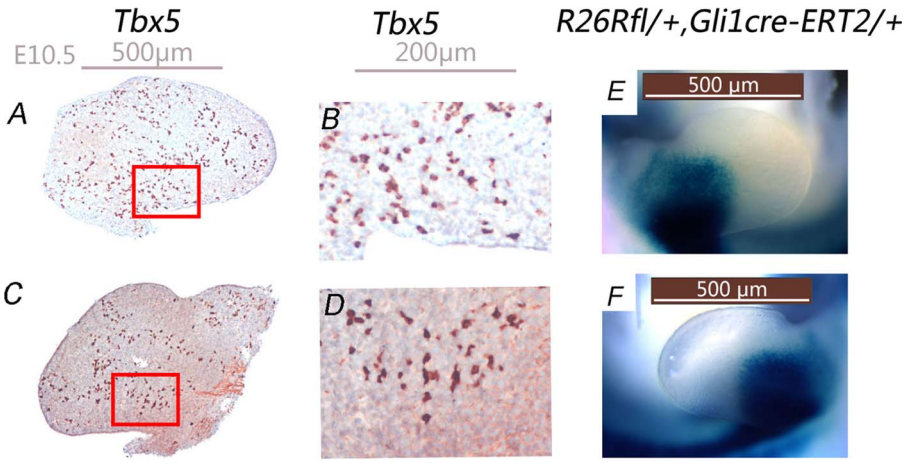

Figure 1. Tbx5 expression in the developing limb overlapped with the location of the Hh-signaling receiving limb precursors. (**A–D**) Tbx5 expression was detected in the developing limb in wild-type mouse embryos by IHC at E10.5. Red frames indicate the enlarged images shown in B and D. (**E–F**) LacZ staining of Gli1-expressing cells in the developing limb in *R26R*$^{fl/+}$; *Gli1-CreER*$^{T2/+}$ embryos at E10.5. The embryos were administered TMX at E7.5 and E8.5.

displayed oligodactyly at this stage to evaluate whether this digit abnormality was associated with enhanced apoptosis at E12.5.

Tbx5 deletion promoted proliferation of autopod mesenchymal cells

We hypothesized that Tbx5 might be required for autopod mesenchymal cell proliferation, whose disruption is closely related to polydactyly or oligodactyly. We assessed proliferation through IHC staining of phosphorylated H3S10, which marks cells in the G2-M phase. The total number of positive cells in the autopod mesenchyme was counted in three serial mid-sections and analyzed for significant differences between the *Tbx5*$^{fl/fl}$;*Gli1-CreER*$^{T2/+}$ embryos and the *Tbx5*$^{fl/+}$ embryos. At E11.5, the number of proliferating autopod mesenchymal cells in *Tbx5*$^{fl/fl}$;*Gli1-CreER*$^{T2/+}$ embryos was significantly greater than that in *Tbx5*$^{fl/+}$ embryos (Fig. 4A and B, 195 ± 13 vs. 120 ± 19, $P = 0.00027$). At E12.5, most H3S10+ cells were located within the interdigit mesenchymal region. Compared with the *Tbx5*$^{fl/+}$ embryos, the *Tbx5*$^{fl/fl}$;*Gli1-CreER*$^{T2/+}$ embryos with polydactyly, but not those with normal digits, had more proliferating cells present within the most anterior peridigit mesenchymal region (Fig. 4C and D, red circle, 40 ± 8 vs. 19 ± 2, $P = 0.0048$). Interestingly, the number of the proliferating cells within the most posterior peridigit mesenchymal region of the *Tbx5*$^{fl/fl}$;*Gli1-CreER*$^{T2/+}$ handplate was similar to that of the *Tbx5*$^{fl/+}$ embryos (Fig. 4C and D, pink circle, 39 ± 4 vs. 39 ± 3, $P = 0.88$). The number of H3S10-positive cells in the middle region of the *Tbx5*$^{fl/fl}$;*Gli1-CreER*$^{T2/+}$ handplate was also significantly elevated in embryos with polydactyly but not normal digits.

Tbx5 deletion resulted in extension of Hh-receiving precursor cells toward the anterior mesenchyme of the limb

To examine the cellular mechanism through which Tbx5 KO caused digit malformation, we tracked the migration of Hh-receiving limb precursors via GIFM, with induction by TMX administration at E7.5 and E8.5, in *R26R*$^{fl/+}$;*Tbx5*$^{fl/fl}$;*Gli1*$^{Cre\text{-}ERT2/+}$ embryos and littermate control embryos. At E10.5, β-galactosidase-positive cells were observed at the proximal–posterior limb bud of the *R26R*$^{fl/+}$;*Gli1*$^{Cre\text{-}ERT2/+}$ embryos (Fig. 5A and A′). The region of β-galactosidase-positive cells in *R26R*$^{fl/+}$;*Tbx5*$^{fl/+}$;*Gli1*$^{Cre\text{-}ERT2/+}$ embryos was similar to that in *R26R*$^{fl/+}$;*Gli1*$^{Cre\text{-}ERT2/+}$ embryos (Fig. 5B and B′). However, that region extended to a more anterior region of the limb bud in the *R26R*$^{fl/+}$;*Tbx5*$^{fl/fl}$;*Gli1*$^{Cre\text{-}ERT2/+}$ embryos (Fig. 5C and C′).

Ptch1 was identified as a direct downstream target of Tbx5 in the developing limb

Shh is required for development of both the posterior–distal limb skeleton and the posterior digits in vertebrate animals (33–35). Our previous study has reported that Tbx5 positively regulates the activity of Hh-signaling in the splanchnic mesoderm during early-stage heart development (29). Thus, we aimed to address the potential interaction between Tbx5 and Hh-signaling in limb development. E10.5 limb buds were collected for RNA extraction and RT-PCR evaluation to determine the key modulator genes involved in Hh-signaling. Expression changes were observed in several genes, including downregulation of *Ptch1* and upregulation of *Smo* and *Gli1* in the *Tbx5*$^{fl/fl}$;*Gli1-CreER*$^{T2/+}$ versus the *Tbx5*$^{fl/+}$ embryos (Fig. 6A), thus suggesting overall Hh-signaling activation in the limb in *Tbx5*$^{fl/fl}$;*Gli1-CreER*$^{T2/+}$ embryos.

Our previous report has shown that *Gas1*, a mediator of Hh-signaling, is a downstream target of Tbx5 in the SHF (29). Therefore, we first tested weather *Gas1* was also a Tbx5 target in the developing limb. Tbx5-response elements were evaluated by ChIP-qPCR with primers covering the previously reported genomic regions (29) (Table 2) and genomic DNA extracted from both the microdissected E9.5 SHF and the E10.5 limb bud. We confirmed one Tbx5-binding site (Gas1-3) in the SHF. This result was consistent with our previously reported data from luciferase reporter assays (29). However, Tbx5 occupancy at the same site in the limb bud was not observed (Fig. 6B). The other two potential sites (Gas1-1 and Gas1-2) were not responsive to Tbx5 in either E9.5 SHF or the limb bud.

The downregulation of *Ptch1* led us to further address whether this gene might be a direct downstream target of Tbx5. We bioinformatically interrogated *Ptch1* loci for potential Tbx5-response elements. We used the overlap of evolutionary conservation and Tbx5 occupancy at a conserved Tbx5-binding

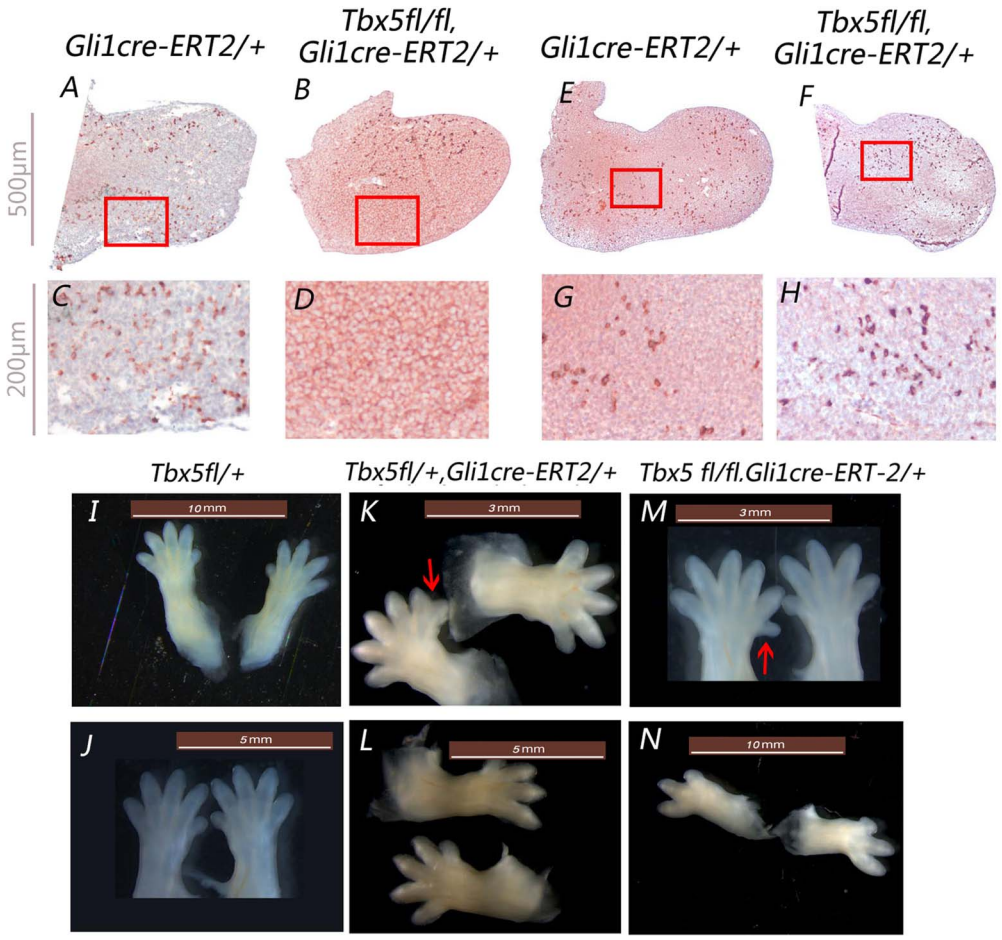

Figure 2. Disruption of Tbx5 expression in Hh-receiving limb precursors resulted in digit defects. (**A–H**) Tbx5 expression in the developing limbs of mouse embryos was detected by IHC at E10.5 (A–D) and at E11.5 (E–H). Magnification: A–F, ×100; C–H, ×400. (**I–N**) Histology of the Tbx5 transgenic mouse embryo limb at E14.5.

Table 1. Incidence of digit defects in Tbx5 mutant embryos (TMX at 7.5 and 8.5)[a]

Genotype	Polydactyly/ oligodactyly	Total defects	Total embryo	vs. control	*P* value
Conditional Tbx5 mutant embryos					
Tbx5$^{fl/+}$;*Gli1-CreER*$^{T2/+}$	7/2	9	82	*Tbx5*$^{fl/+}$ (5/165)	.011
Tbx5$^{fl/fl}$; *Gli1-CreER*$^{T2/+}$	50/10	60	111	*Tbx5*$^{fl/+}$ (5/165)	.000
Smo – *Tbx5* compound mutant embryos					
Tbx5$^{fl/+}$;*Smo*$^{fl/+}$;*Gli1-CreER*$^{T2/+}$ Forelimb	0/0	0	44	*Smo*$^{fl/+}$;*Gli1-CreER*$^{T2/+}$ (0/35)	1
				Tbx5$^{fl/+}$;*Gli1-CreER*$^{T2/+}$ (9/82)	.023
Tbx5$^{fl/+}$;*Smo*$^{fl/+}$;*Gli1-CreER*$^{T2/+}$ Hindlimb	0/0	0	44	*Smo*$^{fl/+}$;*Gli1-CreER*$^{T2/+}$ (0/35)	1
				Tbx5$^{fl/+}$;*Gli1-CreER*$^{T2/+}$ (0/82)	1
Tbx5$^{fl/+}$;*SmoM2*$^{fl/+}$;*Gli1-CreER*$^{T2/+}$ Forelimb	7/0	7	39	*SmoM2*$^{fl/+}$;*Gli1-CreER*$^{T2/+}$ (3/29)	.381
				Tbx5$^{fl/+}$;*Gli1-CreER*$^{T2/+}$ (9/82)	.290
Tbx5$^{fl/+}$;*SmoM2*$^{fl/+}$;*Gli1-CreER*$^{T2/+}$Hindlimb	11/0	11	39	*SmoM2*$^{fl/+}$;*Gli1-CreER*$^{T2/+}$ (12/29)	.288
				Tbx5$^{fl/+}$;*Gli1-CreER*$^{T2/+}$ (0/82)	.000

[a]Significance in digit defects incidence between Tbx5 mutant embryos and littermate controls was analyzed by χ^2 test.

sequence in HL-1 cells (36) and found two potential Tbx5-binding sites (Ptch1-1 and Ptch1-2) within the promoter region of *Ptch1* (Fig. 6C and Table 1). This conserved Tbx5-binding site was confirmed by our ChIP-PCR analysis. The enrichment in Ptch1-1 and Ptch1-2, but not the negative control regions (Ptch1-neg) either upstream or downstream (Tbx5-Fr1 and Tbx5-Fr3), was observed in Tbx5-precipitated DNA fragments extracted from both the microdissected SHF and the E10.5 limb buds of the wild-type embryos (Fig. 6D).

Proper expression of GLI3 protein has been found to specify limb digit number and identity (3,5,37,38). In our study, we observed no changes in expression intensity or expression patterning of *Gli3* in the limb in *Tbx5*$^{fl/fl}$;*Gli1-CreER*$^{T2/+}$ embryos compared with *Tbx5*$^{fl/+}$ embryos via either RT-PCR or ISH

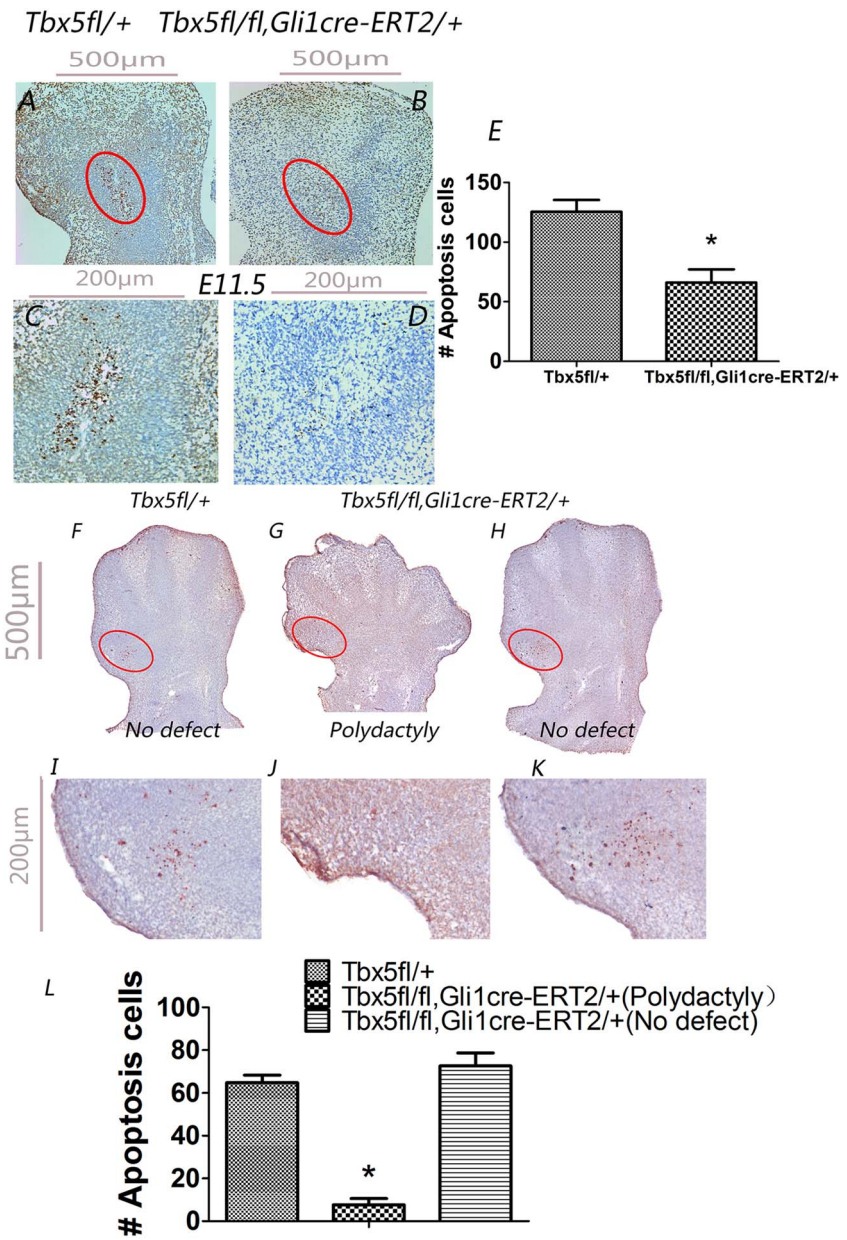

Figure 3. Tbx5 deletion inhibited the apoptosis of the autopod mesenchymal cells that was associated with polydactyly. (**A–D**) TUNEL staining in both *Tbx5*$^{fl/fl}$; *Gli1-CreER*$^{T2/+}$ embryos and control embryos at E11.5. Magnification: ×100 (A and B) and ×400 (B and D). (**E**) Quantification of apoptotic cells of the developing limb at E11.5. Data are presented as mean ± SE, *$P < 0.05$, $n = 3–5$. (**F–K**) TUNEL staining in both *Tbx5*$^{fl/fl}$; *Gli1-CreER*$^{T2/+}$ embryos and control embryos at E12.5. The image panels from I to K are the enlarged images of the circled regions in panels F to H. Magnification: ×40. (**L**) Quantification of apoptotic cells of the developing limb at E12.5. Data are presented as mean ± SE, *$P < 0.05$, $n = 3–5$.

(Fig. 6A and E). Because the expression of *Gli3* does not reflect the changes in the ratio of Gli3A and Gli3R, we therefore measured the expression of the Gli3 downstream gene *Jag1* (39). The expression of *Jag1*, which encodes the Notch ligand, was low in the posterior mesenchyme in wild-type forelimbs, and the expression did not overlap with the ZPA. Strikingly, the *Jag1* expansion extended into the anterior mesenchyme of the *Tbx5*$^{fl/fl}$; *Gli1-CreER*$^{T2/+}$ embryos at E10.5 (Fig. 6E).

We further examined the expression of *Hand2*, a known transcription factor interacting with Gli3, thus further restricting its activation within the posterior limb mesenchyme. In *Tbx5*$^{fl/+}$ mouse embryos, *Hand2* expression was observed at the posterior limb mesenchyme and the mesenchyme of the progress zone (Fig. 6F, left panels). Interestingly, *Hand2* expression in the mesenchyme of the progress zone was lost in the *Tbx5*$^{fl/+}$;*Gli1-CreER*$^{T2/+}$ limb buds (Fig. 6F, middle panels). In the *Tbx5*$^{fl/fl}$;*Gli1-CreER*$^{T2/+}$ limb, the expression of *Hand2* was clearly limited to only the posterior limb mesenchyme (Fig. 6F, right panels).

Recent studies have established that the HoxD family genes (Hoxd10–Hoxd13 and Hoxa13) play an important role in organizing the digital pattern (40). We performed RT-PCR of E10.5 limb buds to assess the molecular regulation of the digital pre-pattern of limbs in *Tbx5*$^{fl/fl}$;*Gli1-CreER*$^{T2/+}$ versus littermate control *Tbx5*$^{fl/+}$ embryos. The expression of *Hoxd10*, *Hoxd11*, *Hoxd12* and *Sox9* was significantly lower in the E10.5 limb buds in *Tbx5*$^{fl/fl}$;*Gli1-CreER*$^{T2/+}$ embryos than in littermate control *Tbx5*$^{fl/+}$ embryos (Fig. 6F), thus suggesting a disruption of digit pre-patterning.

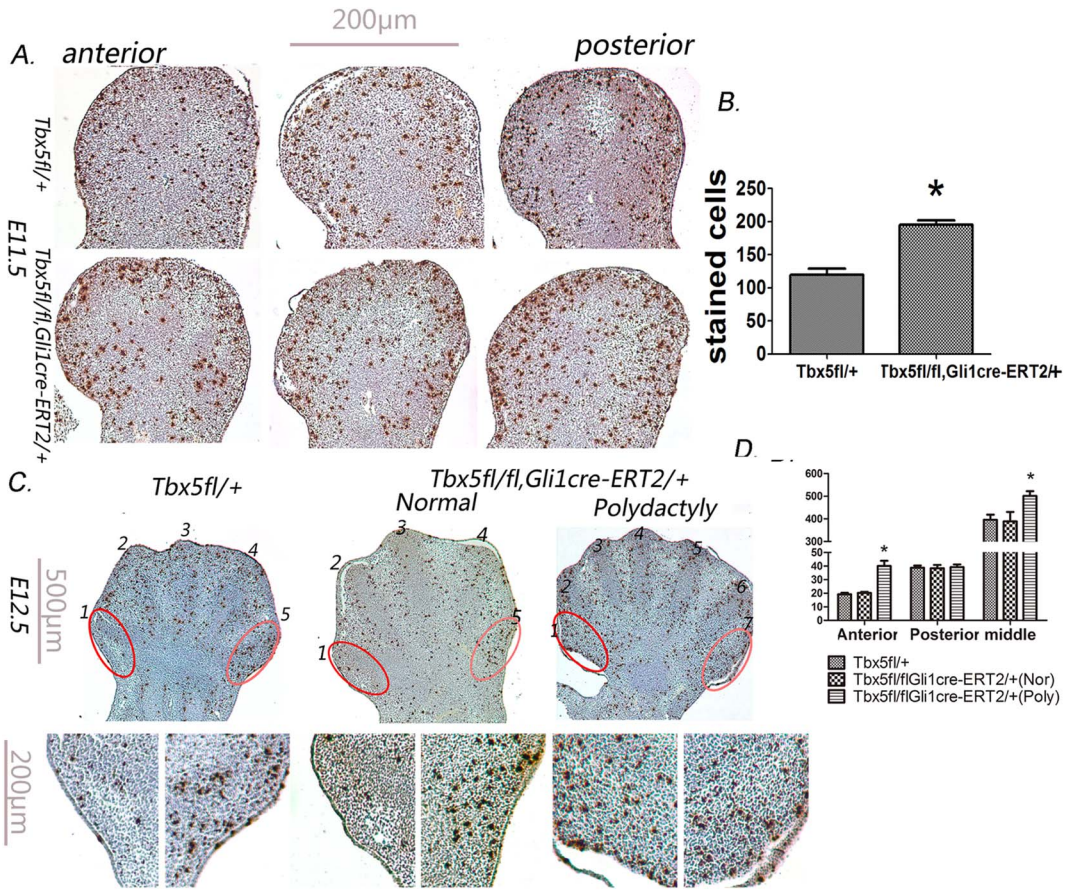

Figure 4. Tbx5 deletion promoted proliferation of autopod mesenchymal cells. (**A**) BrdU staining in both *Tbx5*$^{fl/fl}$; *Gli1-CreER*$^{T2/+}$ embryos and control embryos at E11.5. This figure shows similar sections of the limb from three different embryos in each group. Magnification: ×100. (**B**) Quantification of BrdU-labeled cells from three serial mid-sections of the limb. Data are presented as mean ± SE, $n = 3$–5, *$P < 0.05$. (**C**) BrdU staining in both *Tbx5*$^{fl/fl}$; *Gli1-CreER*$^{T2/+}$ embryos (right and middle panels) and control embryos (left panel) at E12.5. The red circle indicates the anterior region of the handplate, and the orange circle indicates the posterior region of the handplate. Circled area is enlarged in the lower panel. (**D**) Quantification of BrdU-labeled cells counted from the posterior, anterior and middle regions of the handplate from three serial middle sections of the limb. Data are presented as mean ± SE, $n = 3$–5, *$P < 0.05$, Student's *t* test.

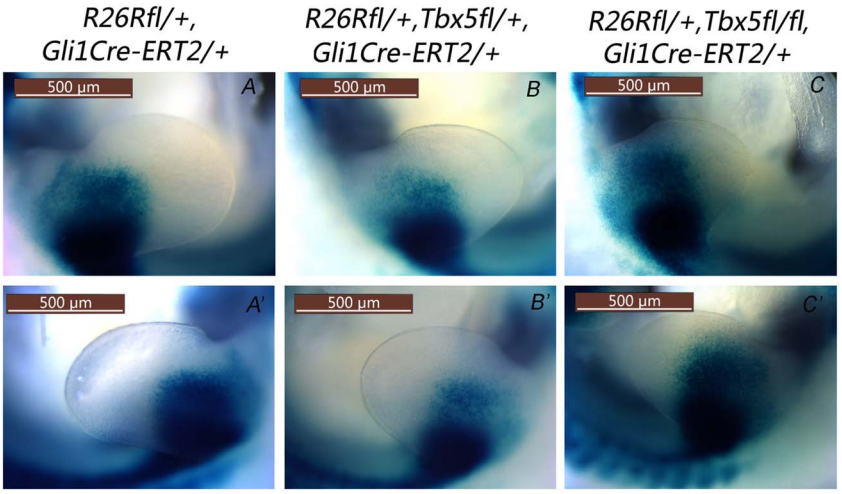

Figure 5. Tbx5 deletion resulted in extension of Hh-receiving precursor cells toward the anterior mesenchyme of the limb. (**A**–**C** and **A′**–**C′**) LacZ staining of Gli1-expressing cells in the developing limb in *R26R*$^{fl/+}$; *Gli1*$^{Cre\text{-}ERT2/+}$ (A: left limb and A′: right limb), *R26R*$^{fl/+}$; *Tbx5*$^{fl/+}$;*Gli1*$^{Cre\text{-}ERT2/+}$ (B: left limb and B′: right limb) and *R26R*$^{fl/+}$; *Tbx5*$^{fl/fl}$;*Gli1*$^{Cre\text{-}ERT2/+}$ (C: left limb and C′: right limb) embryos at E10.5. The embryos were administered TMX at E7.5 and E8.5.

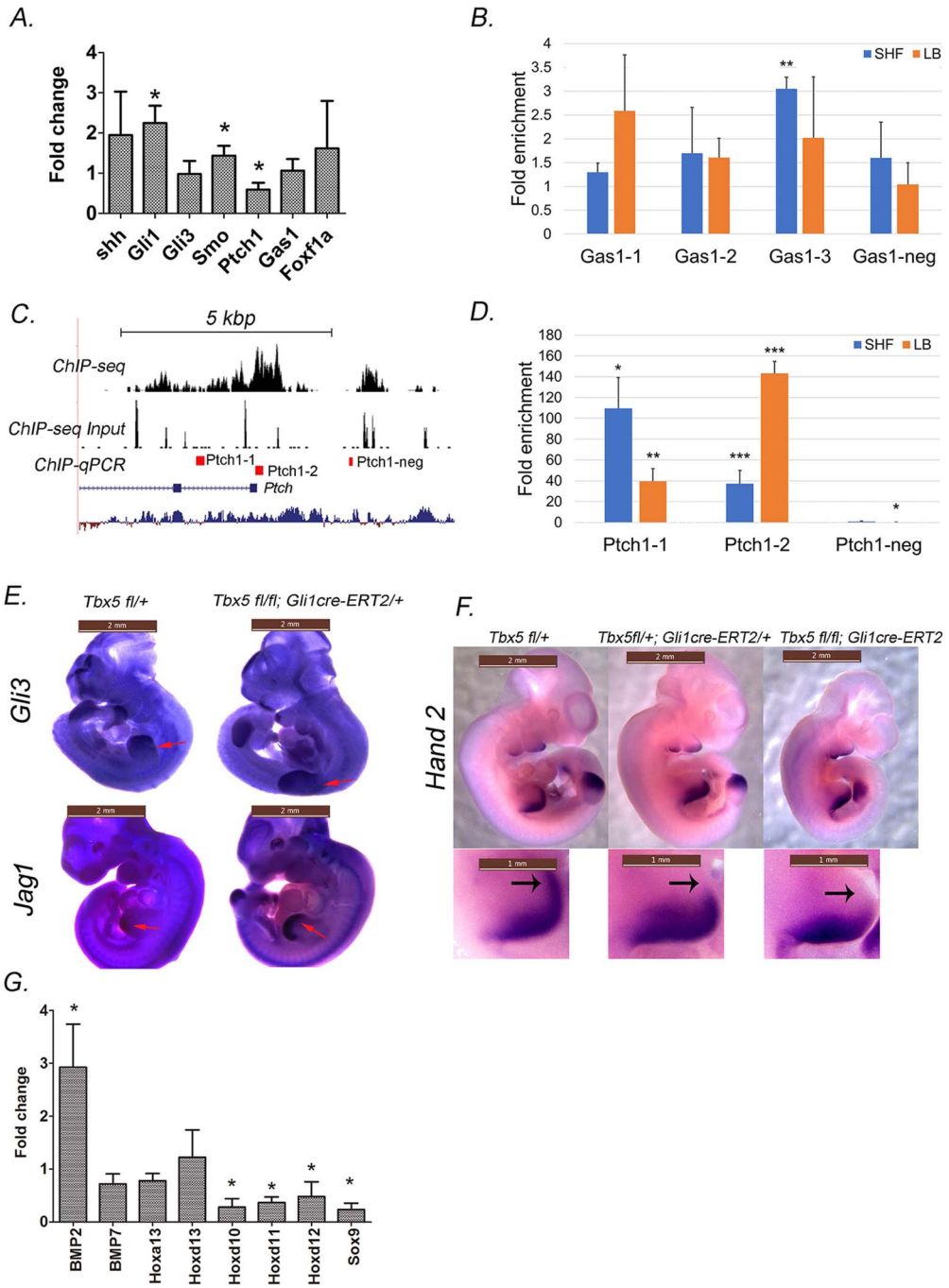

Figure 6. Tbx5 negatively regulated Hh-signaling in the limb bud. (**A**) Expression of key Hh-signaling genes in the limb bud in E10.5 *Tbx5*$^{fl/fl}$; *Gli1-CreER*$^{T2/+}$ and control embryos was measured by real-time PCR. The data are expressed as fold change over control embryos. (**B**) *Tbx5* binds to a *Tbx5* responsive *Gas1* genomic fragment in the SHF, as determined by ChIP-PCR. The *Tbx5*-responsive DNA fragments extracted from the E9.5 SHF and the E10.5 limb bud were immunoprecipitated with anti-*Tbx5* antibody and were amplified by real-time PCR. (**C**) Location of potential Tbx5-binding regions (red bar) adjacent to *Ptch1* in the genome browser. See also Table 2. (**D**) *Tbx5* binds to a *Tbx5* responsive *Ptch1* genomic fragment in both the limb bud and the SHF, as determined by ChIP-PCR. The *Tbx5*-responsive DNA fragments extracted from the E9.5 SHF and the E10.5 limb bud were immunoprecipitated with anti-*Tbx5* antibody and were amplified by real-time PCR. (**E**) Expression of *Gli3* and *Jag1* analyzed by *in situ* hybridization on whole mount *Tbx5*$^{fl/fl}$; *Gli1-CreER*$^{T2/+}$ and control embryos at E10.5. The red arrows indicate the expression in the forelimb bud. (**F**) Expression of *Hand2*, analyzed by *in situ* hybridization on whole mount *Tbx5*$^{fl/fl}$; *Gli1-CreER*$^{T2/+}$ and control embryos at E10.5. The black arrow indicates expression in the forelimb bud. (**G**) Expression of key genes involved in digit identity in the limb bud of E10.5 *Tbx5*$^{fl/fl}$; *Gli1-CreER*$^{T2/+}$ and control embryos, as measured by real-time PCR. The data are expressed as fold change over control embryos. Data are presented as mean ± SE, $^{*}P < 0.05$, $^{**}P < 0.01$, $^{***}P < 0.001$, $n = 3–5$.

Table 2. Genomic regions of Ptch1 and Gas1 assessed by ChIP-qPCR[a]

	Amplified region	Primer sequences
Ptch1-1	chr13: 63565495–63565660	F: 5′-CCGGCGGCGTTACCAGC-3′ R: 5′-ACGGCCGCAGCACCCG-3′
Ptch1-2	chr13: 63566782–63566860	F: 5′-AGCAAATACTGGGAGGTCCG-3′ R: 5′-ACACACTGGCGCACTATCC-3′
Ptch1-neg	chr13: 63567588–63567662	F: 5′-CGGGATTCTGCTACGTCCTA-3′ R: 5′-TTGACTCCTCACTACTCCGGT-3′
Gas1-1	chr13: 60176246–60176431	F: 5′-GTTGAAAAGCTTGCCGCAGTA-3′ R: 5′-GACGAACACTGCAGGTCCAC-3′
Gas1-2	chr13: 60177033–60177198	F: 5′-GTCCGGTAGACGGTTGGAG-3′ R: 5′-CCAGAGCTGCGAAGTGCTAC-3′
Gas1-3	chr13: 60176893–60177052	F: 5′-AAAGTTTGTCCGAGTTCCGC-3′ R: 5′-CCTCCAACCGTCTACCGGAC-3′
Gas1-neg	chr13: 60175035–60175216	F: 5′-CCTAGATGGCAGTACCGAGC-3′ R: 5′-GGGGCTTCCCCGAAATTACA-3′

[a]All genomic coordinates are shown for mouse genome build mm10.

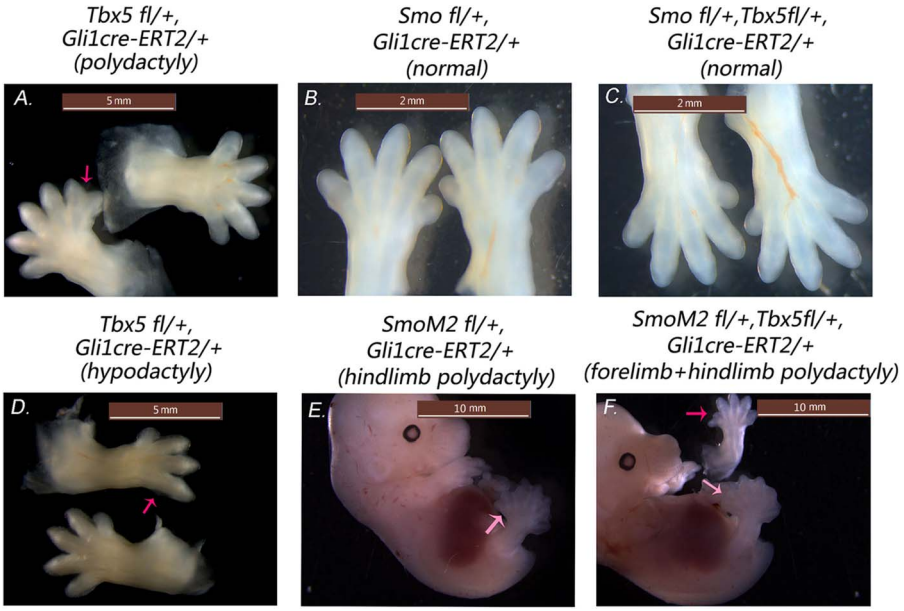

Figure 7. Downregulation of Hh-signaling rescued the forelimb defects in *Tbx5*$^{fl/fl}$; *Gli1-CreER*$^{T2/+}$ embryos. (**A–F**) Histology of the Tbx5 transgenic mouse embryo limb at E14.5. The red arrow indicates forelimb defects, and the pink arrow indicates hindlimb defects.

Downregulation of Hh-signaling rescued the limb defects of *Tbx5*$^{fl/fl}$;*Gli1*$^{Cre\text{-}ERT2/+}$ embryos

Because Tbx5 physically occupied the *Tbx5*-responsive region in the *Ptc1* locus in the limb mesenchyme, we sought to determine whether Tbx5 might functionally inhibit Hh-signaling in digit development. We performed a genetic study by creating embryos with compound heterozygous knockdown of *Tbx5* and *Smoothened*, the latter of which encodes the obligate hedgehog receptor (*Smo*$^{fl/+}$;*Tbx5*$^{fl/+}$;*Gli1-CreER*$^{T2/+}$). As expected, no limb defects were observed at E14.5 in *Smo*$^{fl/+}$;*Gli1*$^{Cre\text{-}ERT2/+}$ embryos (0/35), whereas 15.9% (13/82) of the *Tbx5*$^{fl/+}$;*Gli1-CreER*$^{T2/+}$ littermate control embryos displayed dactyly problems (Fig. 7A). Importantly, compound heterozygous *Tbx5* and *Smo* rescued the dactyly problems observed in the forelimb in *Tbx5*$^{fl/+}$;*Gli1-CreER*$^{T2/+}$ embryos at E15.5 (Fig. 7C, 0/44 vs. 13/82, $P = 0.0226$).

We next combined conditional dominant loss of Tbx5 in Hh-receiving cells with *Gli1:Cre*-dependent expression of SmoM2, a constitutively active Smo mutant (41). In *SmoM2*$^{fl/+}$;*Gli1-CreER*$^{T2/+}$ mouse embryos, we observed polydactyly at both the forelimb and the hindlimb, with a higher ratio in the hindlimb (Fig. 7E, 3/29 in the forelimb vs. 13/29 in the hindlimb, $P = 0.0079$). Combining Tbx5 knockdown with Hh-signaling overactivation did not rescue the forelimb defects of either the *SmoM2*$^{fl/+}$;*Gli1-CreER*$^{T2/+}$ ($P = 0.3812$) or the *Tbx5*$^{fl/+}$;*Gli1-CreER*$^{T2/+}$ ($P = 0.2899$) mouse embryos at E15.5 (Fig. 7F, red arrow). Because Tbx5 does not play roles in hindlimb development, we did not observe incidence changes of hindlimb polydactyly of the *SmoM2*$^{fl/+}$;*Tbx5*$^{fl/+}$;*Gli1-CreER*$^{T2/+}$ (11/39 vs. 12/29, $P = 0.2883$), as expected (Fig. 7F, pink arrow).

Discussion

One of the characteristics of HOS is that the upper-extremity malformations are fully penetrant, and digit abnormality is highly prevalent. Previous studies have demonstrated that Tbx5 positively regulates Hh-signaling activity in the SHF, thereby

influencing atrial septation (29,42). Recent elegant study has used a Tbx5 hypomorphic mouse model to recapitulate the HOS phenotype that the defects are more severe in their left arm than right and to explain why (43). However, no vertebrate model recapitulates the limb-heart defects with TBX5 haploinsufficiency. Although previous studies have shown that *Tbx5* is crucial for forelimb initiation (20,21,23,44) and is an important regulator of thumb length (25,28), it was unknown whether Tbx5 is crucial for digit identity. Our study provides the first report of a Tbx5 haploinsufficient mouse model that recapitulates both the dactyly defects and the heart defects of HOS in humans, although the penetration for dactyly defect is lower in our model than in human patients.

Although previous studies have disclosed the requirement of Tbx5 for limb development, the cell lineage that harbors the dosage sensitive requirement for Tbx5 in digit identity is not identified. By deletion of Tbx5 induced at specific times in Gli1+ cells, we were able to knock down the Tbx5 expression in some of the Hh responders (Gli1+) between E8 and E10.5 which further caused the digit abnormalities. Our results suggest that a narrow time window and a subpopulation of Hh-receiving precursor cells are necessary and that Tbx5 is crucial, for formation of the normal number of digits during limb development. Notably, this short time window overlaps with the previously reported window in which SHF cardiac precursors are required for atrial septation (29). More to be noted, even though we used the Cre-inducible *lacZ* reporter *R26R* (30) with *Gli1cre:ERT2* to create Tbx5 haploinsufficiency, we have no evidence to conclude if the subpopulation of Hh responders were specifically Gli1+ cells, because Gli1 and Gli3 expression overlaps during the time period with TMX induction (45).

Our data support a mechanism through which digit identity requires Tbx5's negative regulation of Hh-signaling in the limb bud. The Gli3R:Gli3A gradient along the AP axis is important for digit development (8). Notably, an increase in digit number in the forelimb together with posterior re-specification of the anterior forelimb has been reported to occur after conditional ablation of functional *Ptch1*, thus suggesting that *Ptch1* is a crucial determinant of asymmetry and digit number in vertebrate limbs (46). Here, we showed decreased expression of *Ptch1* in the E10.5 limb bud and further identified two Tbx5-responsive regulatory regions. These data provide molecular evidence that *Ptch1* is a downstream target of Tbx5, suggesting an overactivation of Hh-signaling in the limb bud in Tbx5 haploinsufficient embryos. In agreement with it, the Tbx5 haploinsufficient limb bud enhanced the expression of *Gli1* and *Smo* detected by real-time PCR. In addition, although the Gli3 mRNA expression pattern was unchanged in Tbx5 mutant embryos, the expression of *Jag1*, which acts downstream of Gli3 depression (39), diffused more anteriorly, thereby suggesting a more extended anterior Gli3A expression. Thus, our data provide a working model in which Tbx5 negatively regulates Hh-signaling, through direct transcriptional regulation of Ptch1, resulting in Gli3A repression. Clearly, the Tbx5-*Hh*-signaling cascade is biologically functional during digit identity: the digit abnormalities in the Tbx5 mutant embryo were rescued by downregulation, but were severer by constitutive activation, of Hh-signaling through conditional ablation of functional *Smo*.

Furthermore, our data suggest that Tbx5 positively regulates cell apoptosis and negatively regulates cell proliferation during handplate development. At the presumptive thumb region *ffp*, GLI3R has been reported to enhance apoptosis and inhibit digit formation (3,5,8). Here, we showed decreased apoptosis of the handplate mesenchyme, especially at the presumptive thumb region, thus suggesting that the increased cell survival in Tbx5 mutant forelimbs might be mediated through the downregulation of Gli3R. We observed an increased number of proliferating cells in the E11.5 handplate mesenchyme and in the E12.5 presumptive thumb region of the Tbx5 mutant embryos. This finding is inconsistent with those from a previous report indicating that the reduced limb size of the Tbx5 mutant embryo is due to a decrease in cell proliferation (25). One possible explanation for these findings is that Tbx5 may inhibit cell proliferation in the handplate mesenchyme through Gli3R at the presumptive thumb region. In fact, active Hh-signaling is required for supporting cell proliferation through its role of positively controlling the expression of genes encoding cell cycle regulators (1,34,47,48).

Clearly, although we demonstrated that Tbx5-Hh-signaling is a major signaling cascade affecting digit identity in Tbx5 mutant embryos, other important signaling pathways and proteins are involved. Hand2 controls *Shh* expression in the polarizing region and is actively repressed in the anterior region of the limb buds, owing to the transcriptional repressor Gli3R (49). In Tbx5 mutant embryos compared with wild-type embryos, *Hand2* expression was restricted to a further posterior region of the forelimb bud, whereas Gli1 expression extended more anteriorly, thus suggesting an interaction between Tbx5-Hh-signaling and Hand2 expression. The decreased expression of HoxD family genes in the forelimb bud also suggested the important roles of factors downstream of Tbx5 or Tbx5-Hh-signaling in re-organizing the digital pattern. Importantly, in agreement with this possibility, disrupted HoxD family gene expression during the patterning stages of limb development has been reported in both Tbx5 mutant embryos and the *Ptch1* mutant embryos (46,50).

Interestingly, Tbx5 negatively regulates Hh-signaling in limb development but plays a positive role upstream of Hh-signaling in the SHF during the same developmental stage (29). This differential activity might be achieved through distinct transcriptional regulatory networks involving Tbx5 and other transcription factors on different gene targets. In the SHF, we identified Gas1, an activator of Hh-signaling, to act downstream of the Hh-signaling pathway. In the limb mesenchyme, similar Tbx5-responsive regulatory regions of *Gas1* are absent, whereas two Tbx5-responsive regions in *Ptch1* were found. However, these two regions were also identified in SHF. Thus, other important components must be required to coordinately interact with Tbx5 in transcriptionally regulating tissue-specific gene targets for activation or repression of Hh-signaling. GATA4, whose mutation also causes atrial septal defects (51,52), physically interacts with TBX5 and NKX2-5, forming macromolecular complexes that activate cardiac gene expression (52,53). We have previously reported that Gata4 and Tbx5 interact and function upstream of Hh-signaling in atrial septation, and we have identified Gata4-responsive genomic regions of *Gli1* (54). Indeed, we observed decreased *Gli1* expression in Tbx5 heterozygous SHF (29). In the limb mesenchyme without Gata4 expression, a direct transcriptional regulatory link from Tbx5 to Gli1 is disrupted. Instead, *Ptch1*, a direct target of Tbx5, plays a major role in repressing Hh-signaling. Similar to Gata4, Gata6 and Tbx5 synergistically transcriptionally activate atrial genes, for example through co-occupying the atrial natriuretic factor promoter (55). Given that Gata6 is a crucial regulator of

Hh-signaling in the limb bud (56), it should be interesting to address whether and how Gata6 and Tbx5 interact in regulating limb development.

In summary, the interaction between Tbx5 and Hh-signaling in digit determination of the forelimb, together with existing knowledge of Tbx5 and Hh-signaling interaction in SHF (29), provides an important missing component for understanding not only limb development but also the molecular and genetic mechanisms underlying HOS.

Materials and Methods

Mouse lines

All mouse experiments were performed in a mixed B6/129/SvEv background. The *Tbx5*$^{fl/+}$, *Gli1-CreER*$^{T2/+}$ and *Smo*$^{fl/+}$ mouse lines were obtained from Dr Ivan Moskowitz Lab (University of Chicago, Chicago). The *SmoM2*$^{fl/+}$ and *R26R*$^{fl/+}$ mouse lines were purchased from the Jackson Laboratory. Mouse experiments were performed according to a protocol reviewed and approved by the Institutional Animal Care and Use Committees of the University of North Dakota and Texas A&M University, in compliance with the US Public Health Service Policy on the Humane Care and Use of Laboratory Animals.

TMX administration and X-gal staining

TMX-induced activation of *CreERT2* was accomplished through oral gavage of mice with two doses of 75 mg/kg TM at E7.5 and E8.5 (57). X-gal staining of embryos was performed as previously described (57).

IHC staining

Standard procedures were used for histology and IHC. IHC was performed with rabbit anti-mouse p-Histone-H3 (H3S10) (Abcam) and rabbit anti-mouse Tbx5 (Santa Cruz). For colorimetric staining, slides were incubated with rabbit ImmPRESS reagent (Vector Labs), developed with a DAB substrate kit (Vector Labs) and counterstained with hematoxylin. For TUNEL staining, an ApopTag Plus Peroxidase In Situ Apoptosis Detection Kit (EMD Millipore) was used.

RNA extraction and RT-PCR

To obtain limb mesoderm for use in quantitative RT-PCR, E10.5 embryos were dissected, and the limb buds were collected in RNAlater and then stored at −20°C until genotyping was completed. Total RNA was extracted from the PSHF regions of mouse embryos with an RNeasy Mini Kit (Qiagen), according to the manufacturer's instructions. Two hundred nanograms of total RNA was reverse transcribed with a SuperScript™ III Reverse Transcriptase Kit from Invitrogen. qPCR was performed with Power SYBR Green PCR master mix from Applied Biosystems. Results were analyzed with the delta-delta Ct method, with *Gapdh* used as a normalization control.

In situ hybridization

In situ hybridization was performed as previously described (29). Specifically, sense and antisense probes were generated with a digoxigenin RNA labeling kit (Roche). Probes were hybridized overnight at 65°C onto E10.5 embryos for whole mount *in situ* hybridization. Digoxigenin-labeled probes were detected with anti-digoxigenin-AP Fab fragments (Roche) and precipitated with BM Purple AP substrate (Roche).

Chromatin immunoprecipitation

The limb buds of E10.5 embryos were collected in cold PBS containing protease inhibitor cocktail (Roche). Approximately 20 pairs of limb buds were pooled as one sample. Tissues were cross-linked with 1% formaldehyde for 15 min at room temperature, and the reaction was terminated with glycine. After being washed several times in PBS, tissues were dissociated by shaking at 37°C for 1–2 h at 100 rpm in collagenase, type II (Gibco) solution. Sonication was performed with a Covaris S220 sonicator to generate an average fragment size of 600 bp. Samples were incubated with anti-Tbx5 antibody (Santa Cruz, sc-1237X) overnight at 4°C, then incubated with Dynabeads Protein G (Life Technologies) for 2 h and washed, and the cross-linking was reversed.

Statistical analysis

Incidence of digit defects was analyzed using chi-squared test (χ^2 test). One-way analysis of variance (ANOVA) was used for assessing the other data including TUNEL assay, H3S10 staining, RT-PCR, ChIP-qPCR, etc. A *P* value less than 0.05 was considered a significant difference. All analyses were carried out using SAS JMP software (SAS Institute Inc., Cary, NC, USA).

Acknowledgements

We greatly appreciate Dr Malcolm P.O. Logan for reading our manuscript and for providing valuable comments.

Conflict of Interest statement. None declared.

Funding

National Institutes of Health (NIH-1R15HL117238 and NIH-1R56HL138479-01 to L.X. and K.Z.)

References

1. Zhu, J., Nakamura, E., Nguyen, M.T., Bao, X., Akiyama, H. and Mackem, S. (2008) Uncoupling sonic hedgehog control of pattern and expansion of the developing limb bud. *Dev Cell*, **14**, 624–632.
2. Chiang, C., Litingtung, Y., Harris, M.P., Simandl, B.K., Li, Y., Beachy, P.A. and Fallon, J.F. (2001) Manifestation of the limb prepattern: limb development in the absence of sonic hedgehog function. *Dev Biol*, **236**, 421–435.
3. Litingtung, Y., Dahn, R.D., Li, Y., Fallon, J.F. and Chiang, C. (2002) Shh and Gli3 are dispensable for limb skeleton formation but regulate digit number and identity. *Nature*, **418**, 979–983.
4. Lopez-Rios, J., Speziale, D., Robay, D., Scotti, M., Osterwalder, M., Nusspaumer, G., Galli, A., Hollander, G.A., Kmita, M. and Zeller, R. (2012) GLI3 constrains digit number by controlling both progenitor proliferation and BMP-dependent exit to chondrogenesis. *Dev Cell*, **22**, 837–848.
5. te Welscher, P., Zuniga, A., Kuijper, S., Drenth, T., Goedemans, H.J., Meijlink, F. and Zeller, R. (2002) Progression of vertebrate

limb development through SHH-mediated counteraction of GLI3. *Science*, **298**, 827–830.
6. Bowers, M., Eng, L., Lao, Z., Turnbull, R.K., Bao, X., Riedel, E., Mackem, S. and Joyner, A.L. (2012) Limb anterior-posterior polarity integrates activator and repressor functions of GLI2 as well as GLI3. *Dev Biol*, **370**, 110–124.
7. Riddle, R.D., Johnson, R.L., Laufer, E. and Tabin, C. (1993) Sonic hedgehog mediates the polarizing activity of the ZPA. *Cell*, **75**, 1401–1416.
8. Wang, B., Fallon, J.F. and Beachy, P.A. (2000) Hedgehog-regulated processing of Gli3 produces an anterior/posterior repressor gradient in the developing vertebrate limb. *Cell*, **100**, 423–434.
9. Kraus, P., Fraidenraich, D. and Loomis, C.A. (2001) Some distal limb structures develop in mice lacking sonic hedgehog signaling. *Mech Dev*, **100**, 45–58.
10. Lewis, P.M., Dunn, M.P., McMahon, J.A., Logan, M., Martin, J.F., St-Jacques, B. and McMahon, A.P. (2001) Cholesterol modification of sonic hedgehog is required for long-range signaling activity and effective modulation of signaling by Ptc1. *Cell*, **105**, 599–612.
11. Yang, Y., Drossopoulou, G., Chuang, P.T., Duprez, D., Marti, E., Bumcrot, D., Vargesson, N., Clarke, J., Niswander, L., McMahon, A. *et al.* (1997) Relationship between dose, distance and time in sonic hedgehog-mediated regulation of anteroposterior polarity in the chick limb. *Development*, **124**, 4393–4404.
12. Basson, C.T., Bachinsky, D.R., Lin, R.C., Levi, T., Elkins, J.A., Soults, J., Grayzel, D., Kroumpouzou, E., Traill, T.A., Leblanc-Straceski, J. *et al.* (1997) Mutations in human TBX5 [corrected] cause limb and cardiac malformation in Holt-Oram syndrome. *Nat Genet*, **15**, 30–35.
13. Li, Q.Y., Newbury-Ecob, R.A., Terrett, J.A., Wilson, D.I., Curtis, A.R., Yi, C.H., Gebuhr, T., Bullen, P.J., Robson, S.C., Strachan, T., Bonnet, D. *et al.* (1997) Holt-Oram syndrome is caused by mutations in TBX5, a member of the Brachyury (T) gene family. *Nat Genet*, **15**, 21–29.
14. Huang, T. (2002) Current advances in Holt-Oram syndrome. *Curr Opin Pediatr*, **14**, 691–695.
15. Wall, L.B., Piper, S.L., Habenicht, R., Oishi, S.N., Ezaki, M. and Goldfarb, C.A. (2015) Defining features of the upper extremity in Holt-Oram syndrome. *J Hand Surg Am*, **40**, 1764–1768.
16. Moens, P., De Smet, L., Fabry, G. and Fryns, J.P. (1993) Holt-Oram syndrome: postaxial and central polydactyly as variable manifestations in a four generations family. *Genet Couns*, **4**, 277–280.
17. Fryns, J.P., Bonnet, D. and De Smet, L. (1996) Holt-Oram syndrome with associated postaxial and central polydactyly. Further evidence for genetic heterogeneity in the Holt-Oram syndrome. *Genet Couns*, **7**, 323–324.
18. Kejariwal, V.K., Misra, P.K., Kumar, A. and Awasthi, S. (1989) Holt-Oram syndrome with polydactyly and ostium primum defect. *Indian Pediatr*, **26**, 1064–1065.
19. Rodriguez-Esteban, C., Tsukui, T., Yonei, S., Magallon, J., Tamura, K. and Izpisua Belmonte, J.C. (1999) The T-box genes Tbx4 and Tbx5 regulate limb outgrowth and identity. *Nature*, **398**, 814–818.
20. Agarwal, P., Wylie, J.N., Galceran, J., Arkhitko, O., Li, C., Deng, C., Grosschedl, R. and Bruneau, B.G. (2003) Tbx5 is essential for forelimb bud initiation following patterning of the limb field in the mouse embryo. *Development*, **130**, 623–633.
21. Ahn, D.G., Kourakis, M.J., Rohde, L.A., Silver, L.M. and Ho, R.K. (2002) T-box gene tbx5 is essential for formation of the pectoral limb bud. *Nature*, **417**, 754–758.
22. Ng, J.K., Kawakami, Y., Buscher, D., Raya, A., Itoh, T., Koth, C.M., Rodriguez Esteban, C., Rodriguez-Leon, J., Garrity, D.M., Fishman, M.C. and Izpisua Belmonte, J.C. (2002) The limb identity gene Tbx5 promotes limb initiation by interacting with Wnt2b and Fgf10. *Development*, **129**, 5161–5170.
23. Rallis, C., Bruneau, B.G., Del Buono, J., Seidman, C.E., Seidman, J.G., Nissim, S., Tabin, C.J. and Logan, M.P. (2003) Tbx5 is required for forelimb bud formation and continued outgrowth. *Development*, **130**, 2741–2751.
24. Duboc, V. and Logan, M.P. (2011) Regulation of limb bud initiation and limb-type morphology. *Dev Dyn*, **240**, 1017–1027.
25. Hasson, P., Del Buono, J. and Logan, M.P. (2007) Tbx5 is dispensable for forelimb outgrowth. *Development*, **134**, 85–92.
26. Fernandez-Teran, M.A., Hinchliffe, J.R. and Ros, M.A. (2006) Birth and death of cells in limb development: a mapping study. *Dev Dyn*, **235**, 2521–2537.
27. Oberg, K.C. (2014) Review of the molecular development of the thumb: digit primera. *Clin Orthop Relat Res*, **472**, 1101–1105.
28. Koshiba-Takeuchi, K., Takeuchi, J.K., Arruda, E.P., Kathiriya, I.S., Mo, R., Hui, C.C., Srivastava, D. and Bruneau, B.G. (2006) Cooperative and antagonistic interactions between Sall4 and Tbx5 pattern the mouse limb and heart. *Nat Genet*, **38**, 175–183.
29. Xie, L., Hoffmann, A.D., Burnicka-Turek, O., Friedland-Little, J.M., Zhang, K. and Moskowitz, I.P. (2012) Tbx5-hedgehog molecular networks are essential in the second heart field for atrial septation. *Dev Cell*, **23**, 280–291.
30. Soriano, P. (1999) Generalized lacZ expression with the ROSA26 Cre reporter strain. *Nat Genet*, **21**, 70–71.
31. Newbury-Ecob, R.A., Leanage, R., Raeburn, J.A. and Young, I.D. (1996) Holt-Oram syndrome: a clinical genetic study. *J Med Genet*, **33**, 300–307.
32. Zuzarte-Luis, V. and Hurle, J.M. (2002) Programmed cell death in the developing limb. *Int J Dev Biol*, **46**, 871–876.
33. Ahn, S. and Joyner, A.L. (2004) Dynamic changes in the response of cells to positive hedgehog signaling during mouse limb patterning. *Cell*, **118**, 505–516.
34. Tickle, C. and Towers, M. (2017) Sonic hedgehog signaling in limb development. *Front Cell Dev Biol*, **5**, 14.
35. Tiecke, E., Turner, R., Sanz-Ezquerro, J.J., Warner, A. and Tickle, C. (2007) Manipulations of PKA in chick limb development reveal roles in digit patterning including a positive role in sonic hedgehog signaling. *Dev Biol*, **305**, 312–324.
36. He, A., Kong, S.W., Ma, Q. and Pu, W.T. (2011) Co-occupancy by multiple cardiac transcription factors identifies transcriptional enhancers active in heart. *Proc Natl Acad Sci U S A*, **108**, 5632–5637.
37. Vokes, S.A., Ji, H., Wong, W.H. and McMahon, A.P. (2008) A genome-scale analysis of the cis-regulatory circuitry underlying sonic hedgehog-mediated patterning of the mammalian limb. *Genes Dev*, **22**, 2651–2663.
38. Hill, P., Gotz, K. and Ruther, U. (2009) A SHH-independent regulation of Gli3 is a significant determinant of anteroposterior patterning of the limb bud. *Dev Biol*, **328**, 506–516.
39. McGlinn, E., van Bueren, K.L., Fiorenza, S., Mo, R., Poh, A.M., Forrest, A., Soares, M.B., Bonaldo Mde, F., Grimmond, S., Hui, C.C., Wainwright, B. and Wicking, C. (2005) Pax9 and Jagged1 act downstream of Gli3 in vertebrate limb development. *Mech Dev*, **122**, 1218–1233.
40. Sheth, R., Marcon, L., Bastida, M.F., Junco, M., Quintana, L., Dahn, R., Kmita, M., Sharpe, J. and Ros, M.A. (2012) Hox genes

regulate digit patterning by controlling the wavelength of a Turing-type mechanism. *Science*, **338**, 1476–1480.
41. Mao, J., Ligon, K.L., Rakhlin, E.Y., Thayer, S.P., Bronson, R.T., Rowitch, D. and McMahon, A.P. (2006) A novel somatic mouse model to survey tumorigenic potential applied to the hedgehog pathway. *Cancer Res*, **66**, 10171–10178.
42. Zhou, L., Liu, J., Olson, P., Zhang, K., Wynne, J. and Xie, L. (2015) Tbx5 and Osr1 interact to regulate posterior second heart field cell cycle progression for cardiac septation. *J Mol Cell Cardiol*, **85**, 1–12.
43. Sulaiman, F.A., Nishimoto, S., Murphy, G.R., Kucharska, A., Butterfield, N.C., Newbury-Ecob, R. and Logan, M.P. (2016) Tbx5 buffers inherent left/right asymmetry ensuring symmetric forelimb formation. *PLoS Genet*, **12**, e1006521.
44. Minguillon, C., Del Buono, J. and Logan, M.P. (2005) Tbx5 and Tbx4 are not sufficient to determine limb-specific morphologies but have common roles in initiating limb outgrowth. *Dev Cell*, **8**, 75–84.
45. Babbs, C., Furniss, D., Morriss-Kay, G.M. and Wilkie, A.O. (2008) Polydactyly in the mouse mutant Doublefoot involves altered Gli3 processing and is caused by a large deletion in cis to Indian hedgehog. *Mech Dev*, **125**, 517–526.
46. Butterfield, N.C., Metzis, V., McGlinn, E., Bruce, S.J., Wainwright, B.J. and Wicking, C. (2009) Patched 1 is a crucial determinant of asymmetry and digit number in the vertebrate limb. *Development*, **136**, 3515–3524.
47. Towers, M., Mahood, R., Yin, Y. and Tickle, C. (2008) Integration of growth and specification in chick wing digit-patterning. *Nature*, **452**, 882–886.
48. Welten, M., Pavlovska, G., Chen, Y., Teruoka, Y., Fisher, M., Bangs, F., Towers, M. and Tickle, C. (2011) 3D expression patterns of cell cycle genes in the developing chick wing and comparison with expression patterns of genes implicated in digit specification. *Dev Dyn*, **240**, 1278–1288.
49. Osterwalder, M., Speziale, D., Shoukry, M., Mohan, R., Ivanek, R., Kohler, M., Beisel, C., Wen, X., Scales, S.J., Christoffels, V.M. *et al*. (2014) HAND2 targets define a network of transcriptional regulators that compartmentalize the early limb bud mesenchyme. *Dev Cell*, **31**, 345–357.
50. Jain, D., Nemec, S., Luxey, M., Gauthier, Y., Bemmo, A., Balsalobre, A. and Drouin, J. (2018) Regulatory integration of Hox factor activity with T-box factors in limb development. *Development*, **145**.
51. Basson, C.T., Bachinsky, D.R., Lin, R.C., Levi, T., Elkins, J.A., Soults, J., Grayzel, D., Kroumpouzou, E., Traill, T.A., Leblanc-Straceski, J. *et al*. (1997) Mutations in human TBX5 [corrected] cause limb and cardiac malformation in Holt-Oram syndrome. *Nat Genet*, **15**, 30–35.
52. Garg, V., Kathiriya, I.S., Barnes, R., Schluterman, M.K., King, I.N., Butler, C.A., Rothrock, C.R., Eapen, R.S., Hirayama-Yamada, K., Joo, K. *et al*. (2003) GATA4 mutations cause human congenital heart defects and reveal an interaction with TBX5. *Nature*, **424**, 443–447.
53. Hiroi, Y., Kudoh, S., Monzen, K., Ikeda, Y., Yazaki, Y., Nagai, R. and Komuro, I. (2001) Tbx5 associates with Nkx2-5 and synergistically promotes cardiomyocyte differentiation. *Nat Genet*, **28**, 276–280.
54. Zhou, L., Liu, J., Xiang, M., Olson, P., Guzzetta, A., Zhang, K., Moskowitz, I.P. and Xie, L. (2017) Gata4 potentiates second heart field proliferation and hedgehog signaling for cardiac septation. *Proc Natl Acad Sci U S A*, **114**, E1422–E1431.
55. Maitra, M., Schluterman, M.K., Nichols, H.A., Richardson, J.A., Lo, C.W., Srivastava, D. and Garg, V. (2009) Interaction of Gata4 and Gata6 with Tbx5 is critical for normal cardiac development. *Dev Biol*, **326**, 368–377.
56. Kozhemyakina, E., Ionescu, A. and Lassar, A.B. (2014) GATA6 is a crucial regulator of Shh in the limb bud. *PLoS Genet*, **10**, e1004072.
57. Hoffmann, A.D., Peterson, M.A., Friedland-Little, J.M., Anderson, S.A. and Moskowitz, I.P. (2009) Sonic hedgehog is required in pulmonary endoderm for atrial septation. *Development*, **136**, 1761–1770.